IEEE Access
Multidisciplinary : Rapid Review : Open Access Journal

Received 4 June 2024, accepted 27 June 2024, date of publication 2 July 2024, date of current version 10 July 2024.

Digital Object Identifier 10.1109/ACCESS.2024.3422073

RESEARCH ARTICLE

Multi–Operator Spectrum and MEC Resource Sharing in Next Generation Cellular Networks

TAHIRA MAHBOOB[1,2], (Member, IEEE), SYED TARIQ SHAH[3], MINSEOK CHOI[4], (Member, IEEE), SANG-HYO KIM[1], (Member, IEEE), AND MIN YOUNG CHUNG[1], (Member, IEEE)

[1]Department of Electrical and Computer Engineering, Sungkyunkwan University, Jangan-gu, Suwon-si, Gyeonggi-do 16419, Republic of Korea
[2]Department of Computer and Software Engineering, Information Technology University of the Punjab, Lahore 54590, Pakistan
[3]School of Computer Science and Engineering, University of Essex, CO4 3SQ Colchester, U.K.
[4]Department of Electronic Engineering, Kyung Hee University, Yongin 17104, Republic of Korea

Corresponding author: Tahira Mahboob (tahira.mahboob@itu.edu.pk)

This work was supported in part by Samsung Research in Samsung Electronics, in part by the National Research Foundation of Korea (NRF) funded by Korean Government [Ministry of Science and ICT (MSIT)] under Grant NRF-2022R1C1C1010766, and in part by the National Research Foundation of Korea (NRF) funded by Korean Government (MSIT) under Grant 2022R1A4A3033401.

ABSTRACT Next-generation cellular networks offer enhanced-mobile broadband, ultra-reliable low latency, and massive machine-type communications. Conventional technology may not meet these demands due to complexity and dynamicity of the network and diverse traffic requirements. To overcome these limitations, resource sharing among network operators is widely studied. The service performance can be improved by leveraging multi-access edge computing (MEC) technology. A mobile user receiving service from virtual network function at the MEC, may experience performance degradation due to lack of resources. To meet the quality of service requirements of users, this paper proposes a multi-operator spectrum and MEC resource sharing scheme. We introduce a user plane function agent at main cloud of the mobile network operator (MNO) that enables inter-operator communications and manages resource sharing requests. Service continuity is enabled by relocating users' associated VNFs considering current resources at the edge network. The proposed scheme has been evaluated using simulations and an experimental testbed. The results show that the proposed scheme reduces network delay, improves network throughput, increases spectrum utilization, increases successful VNF placement ratio, reduces the packet drop ratio, reduces load on edge nodes, and increases revenue for the operator, compared to that of the conventional scheme.

INDEX TERMS Mobile network operators (MNOs), multi–access edge computing (MEC), network function virtualization (NFV), spectrum sharing, virtual network function (VNF) placement.

I. INTRODUCTION

Recently, multi–operator network resource sharing has been studied. The third generation partnership project (3GPP) introduced the concept of sharing the physical network among multiple mobile network operators (MNOs) in its Release 10 [1], [2]. Earlier works on network sharing were focused on radio access network (RAN) sharing, where the infrastructure was shared between MNOs [3], [4], [5]. In Release 14, 3GPP introduced an architecture, named active RAN, for sharing spectrum and core network equipment resources using a network protocol. The protocol included legal, financial, and joint operations agreements between multiple MNOs [2].

Next-generation (NG) wireless communication has introduced enhanced mobile broadband (eMBB), ultra-reliable low latency communications (URLLC) and massive machine-type communications (mMTC). Although, the

The associate editor coordinating the review of this manuscript and approving it for publication was Petros Nicopolitidis.

computational and intelligence capabilities of user equipment (UE) have enhanced significantly, NG services cannot be solely executed in these user devices. To overcome current front-haul and back-haul capacity limitations, dependable solutions are required for appropriate network upgrades and re-modeling of the conventional network architecture.

To overcome these problems of dynamic and complex requirements of NG services, a multi-access edge computing (MEC)-enabled architecture has been proposed in the literature [6]. MEC-enabled architecture incorporates cloud computing capabilities at the network edge. MEC network architecture is supported by virtualization of network services and applications, referred to as virtual network functions (VNFs), and decentralization of computing and network resources. Network function virtualization (NFV) alleviates the need for restricted and fixed placement of network functions (NFs), conventionally implemented in the legacy long term evolution (LTE) network [7].

In an MEC network, user's proximity and required quality-of-service (QoS) can be considered to implement applications and NFs as VNFs at various locations in a distributed system, managed by a centralized NFV orchestrator (NFVO) [8]. Existing works such as [9] have introduced a small cell cloud-enabled LTE network architecture to support mobile offloading. Cloud services have been integrated into mobile network by B. Flavio et al., on an NFV/software-defined networking (SDN) architecture [10]. A centralized core network has been implemented as a distributed architecture by O. Antonio et al. in [11]. In these previous works, though the RAN and infrastructure resources are shared among MNOs. The RAN sharing solutions are fairly complex, information related to the softwarization of the network functionalities and methods of VNF migration are not clearly defined.

In this paper, we propose a multi-operator resource sharing scheme, where the spectrum and MEC resources are shared. The key benefits of the proposed scheme are 1) a less complex spectrum sharing scheme, allowing users to achieve the required QoS in a time coordinated manner. 2) The inter–operator spectrum sharing agent, UPF_G agent, implemented at each the MNO cloud connects to the core network via direct communication link, provides an abstraction layer between multiple operators. 3) The proposed scheme provides spectrum selective and time dependent spectrum and MEC resource sharing among multiple operators.

A UE receiving services from a VNF at MEC, may experience performance degradation, and MEC of another MNO may provide services (VNFs) to the specific user to maintain its quality–of–service (QoS) in a resource shared environment consisting of multiple MNOs. To provide service continuity, MNOs needs to communicate and relocate the services used by UE from the source to the target MEC of another operator. To achieve better network performance, the individual resource requirements of services are taken into account for VNF placements at the MEC network. By utilizing user context information, we propose a method that takes the available RAN resources, the computational and network limitations of MEC network into account, to share resources in a multi-operator environment.

TABLE 1. Table of notations.

Symbol	Value
a_{1r}, a_{2r}, a_{3r}	average downlink throughput at gNB, average network delay at gNB, and candidate gNB buffer size
b_{1r}, b_{2r}	average price per packet (byte), priority of a service
γ and θ	weight values $\in$ (0,1) for pricing and performance metric
X_{ζ_r}, ξ_r	performance metric, pricing metric
Y_r	final score value for resource sharing among MNOs
Y_{th}	threshold value of score Y_r
U_{Cij}	CPU utilization by VNF i at NFV node j
U_{Mij}	RAM utilization by VNF i at NFV node j
U_{Bij}	Link bandwidth utilization by VNF i at NFV node j
U_{Dij}	Disk space utilization by VNF i at NFV node
L_{th}	Load threshold value at the NFV node
L_{ij}	Load on an NFV node j if VNF i is executing on it
δ_U	delay experienced by UE U
δ_{th}	pre-defined tolerable delay threshold

The main contributions of this work are as follows:

- Introducing a user plane function agent, UPF_G, at the main cloud of the NG cellular network, enables inter-operator communications and management of resource sharing among multiple MNOs. The UPF_G, allows granularity and isolation for inter-operator communications.
- At the UPF_G, we introduce an algorithm to select an MNO among a list of candidate MNOs for sharing network resources. It considers selecting the near optimal candidate for sharing the resources considering the current network conditions.
- An efficient VNFs placement scheme is proposed that takes available resources in the MEC network into account, while meeting the individual resource requirements of the VNFs. The efficient deployment of VNFs enables feasible resource utilization, in terms of spectrum utilizations and revenue generation for operators.
- A proof-of-concept is provided by implementing the proposed resource sharing scheme using an emulation tool and simulations. The results indicate that the proposed scheme increases the throughput, reduces the delay, reduces the packet drop ratio, improves the spectrum utilization, reduces the average load on the NFV nodes, increases the VNF placement ratio, and increases the revenue for the operator, compared to that of the conventional scheme.

The rest of the paper is organized as follows. Section II briefly discusses the related works. The proposed scheme is detailed in Section III. In Section IV, we evaluate the performance and explain the simulation, the emulation environment, and the evaluation results. Lastly, we conclude the paper in Section V.

II. RELATED WORKS

Dynamic spectrum sharing has been widely accepted by industry and academia. In release 15 of 3GPP, the 4G LTE

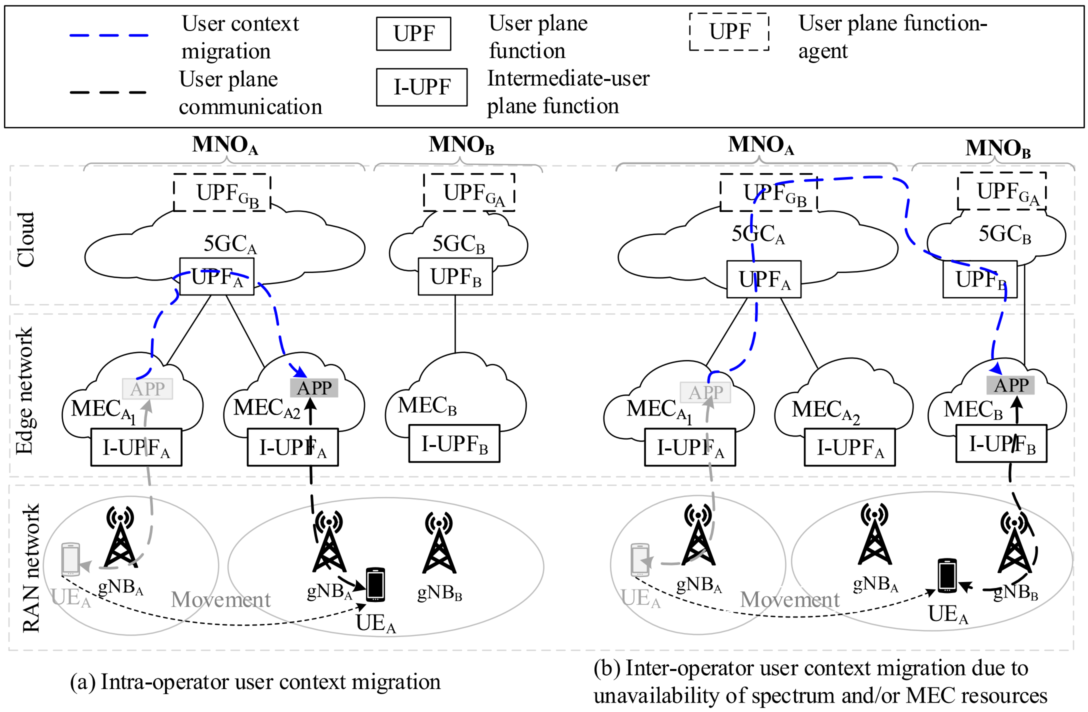

FIGURE 1. An example of the proposed multi-operator resource sharing in NG networks.

and 5G new radio (NR) coexistence in the same frequency band was introduced and accepted during standardization [3]. Spectrum resources could be allocated dynamically between the two types of technologies based on user demands.

Researchers have actively studied resource sharing and multi–operator spectrum sharing methods [4], [5], [12], [13], [14]. Authors in [15] studied spectrum sharing among multiple operators for indoor deployments. The authors use a shared pool spectrum resources and implement a Markov chain Monte Carlo–based algorithm to assign suitable resource blocks to operators In [16], following a game–theoretic approach, the magnitude of sharing between multiple operators is estimated based on the number of favors each operator makes to other operators. Authors in [17], proposed a game–theoretic solution using the generic Markov Chain Monte Carlo method to obtain the maxima of social welfare. To reduce the interference, Q–learning was used to optimize the transmit power of small bases stations. With learning capabilities, each base station does not need to acquire other players' strategies explicitly. The simulation results showed an increase in the long–term expected data rate. These approaches have been proposed mainly for systems with separate agents/objectives that compete for shared resources, whereas licensed–operator networks conventionally have dedicated resources. Moreover, these approaches are based on complex mathematical formulations and optimization methods. Complexity in these solutions increase considering evolving dynamicities in NG networks.

Recently, machine learning has gained attention offering promising solutions for complex and dynamic resource management problems. Luoto et al. considered a mobile network where operators shared a common pool of radio resources [18]. A distributed spectrum allocation algorithm using deep learning based on Gibbs sampling was proposed. Long term fairness of spectrum sharing is ensured without coordination among small cell base stations. However, embedding deep learning modules in network entities for resource management, such as, estimation of resource allocation and/or scheduling decisions, increases computational overhead, which may not be feasible to the operators in practice.

To reduce capital and operational expenditures, while meeting the demands of NG networks, wireless network virtualization has been regarded as a promising paradigm [19], [20]. Network virtualization consists of mainly four components, i.e., the spectrum resources, the network infrastructure, the wireless virtual controller, and the wireless virtual resources/services. Authors in [21], studied the functionality of 3GPP network sharing standardization and analyzed that futuristic networks would require advanced solutions based on virtualization.

The European Telecommunication Standard Institute (ETSI) MEC ISG has worked on standardization efforts for MEC architecture [22], [23], [24]. MEC has been considered as a key component for NG networks [25]. MEC enables storage and computing capabilities at the network's edge to support NG services, backed by intelligent NFs and big data analytics [26]. Also, services requiring high computational demands can be offloaded to the MEC cloud, providing solutions for bandwidth-intensive and low latency applications/services [27]. Furthermore, SDN and network slicing can provide flexibility, ease of implementation and access by users, developers, and content providers for the required services [6], [28], [29].

Dynamic resource management over the edge network, supported by integration of resources and orchestration platform, such as NFV, requires efficient selection and management of computing, storage, and network resources [30], [31]. In this way, the service performance at the MEC is enhanced such that it meets the QoS requirements of the services offered to the mobile users.

From the literature review, we analyzed that most of the resource sharing schemes are based on separate agents/objectives that are implemented based on complex mathematical formulations and optimization solutions. This may not scale feasibly considering evolving dynamicities in NG networks. Also, machine learning and deep learning–enabled resource sharing solutions increase the computational overhead significantly which may not be feasible in practice. Furthermore, VNFs embedding solutions imply that that the MEC network has enough capacity to offer services or not. The individual resource requirements of the VNFs have been ignored and dynamic migration of VNFs has not been considered. To overcome these problems, in this paper, we propose a novel multi–operator spectrum and MEC resource sharing scheme that provides the required service performance to the mobile UEs and improves network efficiency. In addition, the proposed scheme is compared to the conventional scheme, in terms of, throughput at the MNOs under different traffic profiles, packet drop ratio, number of successful VNF placements on the nodes at the MEC network, load on the NFV nodes, revenue opportunity for MNOs, delay, and spectrum utilization [22], [23].

III. PROPOSED SCHEME

The 5G Service Based Architecture (SBA) specified by 3GPP TS 23.501, contains multiple control plane functional entities, like the policy control function (PCF), the session management function (SMF), the application function (AF), and the data plane functional entities such as the user plane function (UPF) [32]. 5G system was introduced to allow a more flexible deployment of the data plane to support edge computing natively. We present a resource sharing scheme for NG cellular networks employing MEC mapping to the 5G system architecture.

In this paper, we consider resource sharing among MNOs. We assume that the UE can subscribe to multiple MNOs. Also, the MNOs have a prior agreement of information exchange about the resource sharing scheme, via a newly defined NF, referred to as, the user plane function agent (UPF_G), present at the main cloud of the MNO. The UE profile and subscription information, such as, subscribed services from each network operator are stored in the unified data repository (UDR) at the subscribed network operator's unified data management (UDM) NF in the 5G Core (5GC) network. A UE receives service from MNO A's MEC, MEC_A, through gNodeB, gNB_A, base stattion in NG networks, as shown in Fig.1(a). The UE service performance may degrade due to the lack of resources. This scenario may result in a disruption in required QoS to the UE. The operators need a suitable resource–sharing scheme to provide users with the required service quality and continuity.

To satisfy the quality–of–service (QoS) requirements of the services offered to the UE, the MEC belonging to another MNO, i.e., MEC_B which is close to the UE's point of attachment (POA) and within the coverage region, may provide spectrum and/or MEC resources. This requires inter–operator migration of user context[1] and placement of associated VNFs from the cloud to the target edge network, as presented in Fig. 1(b). For example, in the case of video streaming service, the service context associated with a UE consists of the requested video file name and the current offset in the file.

The process flow of multi–operator spectrum and MEC resource sharing is presented in Fig. 2. UE is initially associated with MNO_A and receives services through VNFs located at MEC_A. If the QoS of the services offered to the UE goes below a pre–defined threshold value, Q_{th}, the UE may handover. There are two alternative scenarios for handover decisions in this situation; either the UE measures its QoS via a utility program installed on it, such as tcpdump,[2] or the gNB, i.e., gNB_A, serving the UE estimates service performance. Whereas, for the latter case, the gNB measures the QoS of services used by a UE and initiates a forced handover to other MNO, i.e., MNO_B in this case.

For UE initiated resource sharing, the UE is authenticated by the MNO_B's core network, $5GC_B$, following the access request. The target network MNO_B must have sufficient resources to provide the required QoS. To acquire this information, a ''resource requirement request'' message is transmitted to the user plane function agent, UPF_{G_B}, present at the main cloud of MNO_A.The UPF_G is trusted NF for cooperating MNOs and is responsible for inter-operator communication.

The UPF_{G_B} retrieves the UE's currently used services information from the serving MEC, including the name and type of VNFs, the priority of each service, QoS requirements of the services, and duration of services. These service-related information is transmitted to the UPF_{G_B}. A ''resource requirement response'' message is then transmitted to the core network of MNO_B containing this information. If the available resources at the MNO_B is sufficient to meet the resource requirements, the resource sharing request is accepted and a confirmation message is transmitted to gNB_B. Following this, the resource requirement control (RRC)

[1]UE context consists of information, such as, network session information between the service and the UE.

[2]tcpdump executable installed on a UE captures traffic at a specified interface. The captured data can be filtered to evaluate local performance, such as, downlink throughput, of data services.

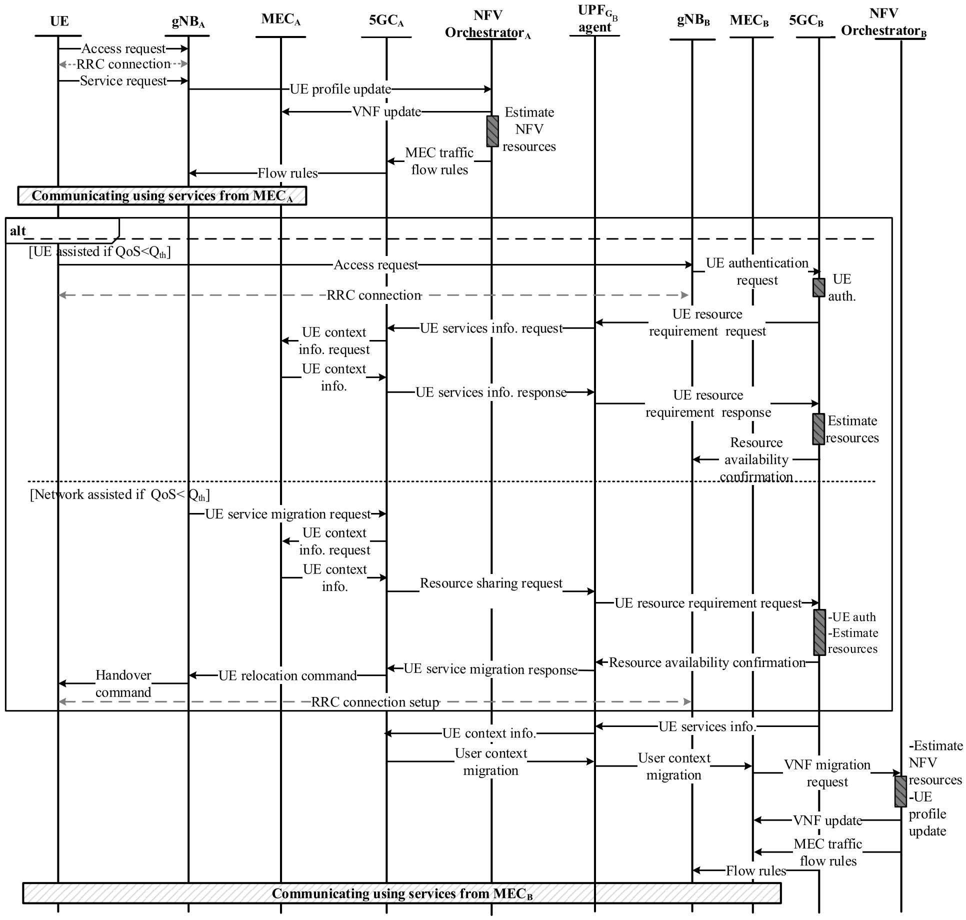

FIGURE 2. The process flow for inter–operator user service migration.

connection is established between the UE and the gNB$_B$. The user context information is then obtained from the MNO$_A$ via the UPF$_{G_B}$ agent.

In case of network-assisted handover, the gNB at the current serving network, measures the service performance and initiates forced handover of the UE to the other network, if the QoS requirements of offered services are not satisfied by the current network. The resource sharing request is transmitted to the target MNO$_B$ via the UPF$_{G_B}$. This resource sharing request message contains the required resources from the target network. Once the UE is authenticated and available resources at the target network satisfy the request, the resource availability confirmation message is transmitted to the UPF$_{G_B}$, which is then forwarded to the 5GC$_A$ of the serving network, MNO$_A$. This initiates a forced handover of UE to the MNO$_B$, via UE relocation message and handover messages transmitted to the concerned gNB and the UE, respectively.

The MEC platform leverages the 5G network architecture and performs the traffic routing and steering function in the UPF. The procedure for user context migration is shown in Fig. 3. In step 1, UE$_A$ service information request message is transmitted from UPF$_{G_B}$ of MNO$_A$. This message is forwarded to the UPF at the MNO$_A$. In step 2, the UPF notifies SMF to request UE$_A$ information. UE$_A$ information is verified at the UDM in step 3. The UDM transmits UE$_A$ information in the response message to the SMF in step 4. In step 5, UE$_A$'s charging records, CDRs, etc., are generated at SMF and transmitted to PCF for storing billing information for UE$_A$. UE$_A$ context information request message is transmitted to MEC$_A$ in step 6. UE$_A$ context information is fetched at the SMF in steps 7 and 8. This retrieved UE$_A$ context information is transmitted to the UPF in step 9. In step 10, the UPF transmits UE$_A$ context information to UPF$_{G_B}$ of MNO$_A$. In step 11, the information of UE$_A$ stored at the orchestrator is updated.

A. DECISION ALGORITHM TO MANAGE MULTI–OPERATOR RESOURCE SHARING REQUESTS

To enable scalability of the proposed multi–operator resource sharing scheme, we introduce a decision algorithm at the UPF$_G$. MNOs sharing their resources within a region are referred to as the candidate MNOs. The algorithm calculates a score value to select an MNO among the candidate MNOs. As shown in Fig. 2, the decision algorithm is executed for a UE initiated service migration scenario when a "UE resource

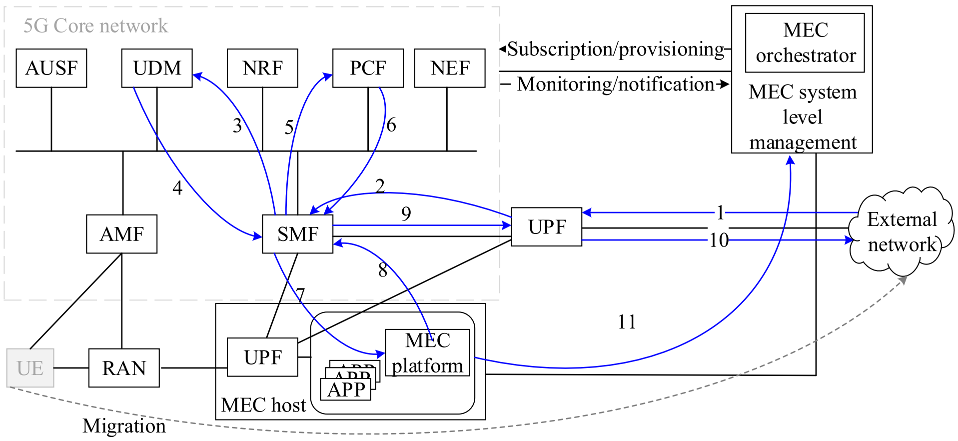

FIGURE 3. The procedure for user context migration in multi–operator resource sharing environment.

requirement request'' message is received at the UPF_G. In the case of network–assisted UE service migration, it is activated when a ''resource sharing request'' message is received at the UPF_G. This initiates the decision algorithm at the UPF_G.

When multiple MNOs share resources under an agreement and have gNBs in proximity, the network-related information is transmitted by UPF_G of an MNO to agents of other MNOs, in pre-defined intervals. This information is stored in a newly defined local database at the 5GC. Accepting a resource sharing request can be decided on two metrics; the performance metric, X_{ζ_r}, and the pricing metric, X_{ξ_r},for gNB r. Both performance and pricing metrics for gNB_r are defined as

$$X_{\zeta_r} = \sum_{p=1}^{3} w_{pr} a_{pr} \tag{1}$$

and

$$X_{\xi_r} = \sum_{q=1}^{2} v_{qr} b_{qr}, \tag{2}$$

where a_{1r}, a_{2r}, and a_{3r} are the average down-link throughput at gNB, the average network delay, and the candidate gNB buffer size for the performance metric, respectively. In the paper, throughput is defined as the amount of data packets transferred from gNB to UE in a pre–defined time duration. Network delay is measured as the time taken to transmit data packets on the outgoing link. Buffer size is calculated as the number of packets stored in the queue at the gNB. These parameters can be obtained using performance monitoring tools [33]. Also, b_{1r} and b_{2r} are the average price per packet (byte) of a service and the priority (user profile specific as per service level agreement (SLA)) of a service, for pricing metric determined by MNO, respectively. In addition, w_{pr} and v_{qr} are the weight values in the range (0, 1) for the performance and pricing parameters, respectively [34].

To select the MNO for resource sharing among candidate MNOs, the final score can be calculated using:

$$Y_r = \gamma X_{\zeta_r} + \theta X_{\xi_r}, \tag{3}$$

where γ and θ are the weight values in the range (0, 1) for performance and price metrics for gNBr, respectively. A resource sharing request can be accepted if Y_r is greater than a threshold value Y_{th}, i.e., $Y_r \geq Y_{th}$, otherwise, the request is forwarded to another MNO in the candidate list having the highest score value.

When a target network accepts a resource sharing request, the next step is to share the spectrum and migrate the required services from the cloud data network, e.g., the Internet, on to the MEC nodes. The services offered to the users are implemented as VNFs on a virtualization platform. The optimal placement of these VNFs on candidate NFV nodes is necessitated. The placement of VNFs, based on resource availability on the NFV nodes in the MEC network, is discussed in the next sub-section.

B. MIGRATION OF SERVICES ON MEC NETWORK

We represent the MEC network architecture with a set of NFV nodes $\mathbb{S} = \{s_1, s_2, \ldots, s_K\}$ and a set of VNFs $\mathbb{V} = \{v_1, v_2, \ldots, v_N\}$, where K are the number of NFV nodes at the MEC network and N are the numbers of different types of VNFs. The placement of VNF on an NFV node is represented by an indicator function, defined as

$$x_{ij} = \begin{cases} 1, & \text{if } v_i \text{ is executing on } s_j \\ 0, & \text{otherwise.} \end{cases} \tag{4}$$

The indicator function for verifying that VNF is present on source NFV node at the cloud network before migration to NFV node at the target MEC network is defined as

$$y_{il} = \begin{cases} 1, & \text{if } v_i \text{ is executing on } s_l \\ 0, & \text{otherwise.} \end{cases} \tag{5}$$

Managing the load on the NFV nodes is essential to avoid inefficient resource utilization. The load on an NFV node, if v_i is placed on s_j, can be calculated as

$$L_{ij} = \alpha U_{C_{ij}} + (1-\alpha)U_{M_{ij}} + U_{B_{ij}} + U_{D_{ij}}, \quad (6)$$

where α is a real number in (0, 1). $U_{C_{ij}}$, $U_{M_{ij}}$, $U_{B_{ij}}$, and $U_{D_{ij}}$ are the CPU (C), RAM (M), link bandwidth (B), and disk space (D) utilizations, respectively. For example, a transcoder type *VNF* may require more computational power, a high value can be assigned to a before placing it on to the target NFV node. Note that it is infeasible to modify the disk space and bandwidth requirements before placement on an NFV node.[3]

We define, $U_{C_{ij}} = c_i/C_{max_j}$, where c_i is the CPU requirement in terms of processor rate for v_i and the maximum capacity, C_{max_j}, of s_j can be represented in hertz (Hz). We define RAM utilization as $U_{M_{ij}} = m_i/M_{max_j}$. Here, m_i is the required RAM for v_i and the maximum capacity of RAM is denoted as M_{max_j} on s_j represented in MBs. $U_{B_{ij}}$ can be defined as $U_{B_{ij}} = \frac{b_i}{B_{max_j}}$, where b_i is the bandwidth requirement for v_i and B_{max_j} is the maximum link capacity expressed in bits per second (bps). Also, $U_{D_{ij}}$ can be defined as $U_{D_{ij}} = \frac{d_i}{D_{max_j}}$, where d_i is the disk space required for v_i and D_{max_j} is the maximum storage available expressed in MBs.

We consider a UE_A is receiving service via MEC_A. If the delay experienced by the UE_A reaches a threshold value, $\delta_U \geq \delta_{th}$, the user may request to handover to the MNO_B. In this case, the user context needs to be migrated to MNO_B. The MEC_B, may not have the UE_A associated VNFs executing on the NFV nodes, therefore; the VNFs need to be migrated from the cloud data network.

The total load on NFV node j in the MEC_B can be calculated as

$$L_j = \sum_{i=1}^{N} L_{ij}x_{ij} \text{ for } j \in \{1, 2, \cdots, K\}. \quad (7)$$

The load on NFV nodes when migrating VNFs on them can be expressed using Integer Linear Programming (ILP). Therefore, we formulate the ILP model as

$$\min_{\alpha} \sum_{j=1}^{K} L_j = \min_{\alpha} \sum_{j=1}^{K} \left\{ \sum_{i=1}^{N} [\alpha U_{C_{ij}} + (1-\alpha)U_{M_{ij}} + U_{B_{ij}} + U_{D_{ij}}]x_{ij} \right\} \quad (8)$$

$$\text{subject to: } \sum_{i=1}^{N} x_{ij}U_{C_{ij}} \leq C_{max_j}, \quad \forall j \in \{1, 2, \cdots, K\}, \quad (9)$$

$$\sum_{i=1}^{N} x_{ij}U_{M_{ij}} \leq M_{max_j}, \quad \forall j \in \{1, 2, \cdots, K\} \quad (10)$$

$$\sum_{i=1}^{N} x_{ij}U_{B_{ij}} \leq B_{max_j}, \quad \forall j \in \{1, 2, \cdots, K\}, \quad (11)$$

$$\sum_{i=1}^{N} x_{ij}U_{D_{ij}} \leq D_{max_j}, \quad \forall j \in \{1, 2, \cdots, K\}, \quad (12)$$

$$\sum_{j \in K} x_{ij} = 1, \quad \forall i \in \{1, 2, \cdots, N\} \quad (13)$$

$$x_{ij} \leq y_{il}, \quad \forall j \in \{1, 2, \cdots, K\}, \quad (14)$$

$$L_j \leq L_{th_j}, \quad \forall j \in \{1, 2, \cdots, K\}. \quad (15)$$

The proposed ILP aims to minimize NFV node loads at the MEC network, as given in Eq. (8). Eq. (9) indicates that the sum of CPU utilizations of all VNFs currently executing on an NFV node should be less than its maximum CPU capacity. In the same way, the sum of RAM utilization of all VNFs currently executing on an NFV node should be less than the RAM size of that node, presented in Eq. (10). In Eq. (11), the sum of BW requirements for all VNFs executing on an NFV node should be less than its total link capacity. In Eq. (12), the sum of disk space required to embed all VNFs on an NFV node should be less than its total storage capacity. In Eq. (13), the constraint ensures that each VNF is assigned to an NFV node. Also, the constraint in Eq. (14) verifies that the VNF is present on the source node at the cloud before it is migrated to the NFV node at the target MEC. is constraint ensures that the VNF is available on the respective cloud network before it is migrated onto the target MEC network. From Eq. (15), the load on s_j is constrained by a pre-defined load threshold value.

The NFV node capabilities and capacities may vary depending on hardware (HW), such as, CPUs, GPUs, FPGAs, and other system specifications [35]. Such a heterogeneous HW environment challenges network administrators to assign the tasks appropriately. Also, resource specifications of computing such as the number of graphical processing units (GPUs), the number of CPU cores, and special FPGAs hardware, may have an affect on the performance of that system. Therefore, as the performance is hardware dependent, a careful determination of the load threshold limit, L_{th_j}, is needed.

1) VNF MIGRATION ALGORITHM

The ILP model formulated for the placement of VNFs on the NFV nodes at the MEC network is a well–known NP–hard problem [36]. Therefore, we propose a heuristic algorithm to place VNFs on NFV nodes at the MEC network, presented in Algorithm 1. We consider a UE receiving service from VNF at an MEC network, associates to another gNB when service performance degrades and continues to receive service from another MEC network. The VNFs and NFV nodes are ordered considering priority and minimum delay, respectively.

In steps 11-31, the VNFs are placed on these NFV nodes closest to the user location among the ones meeting the CPU, memory, bandwidth, and disk storage requirements. If no NFV node satisfies the requirements, the algorithm searches for directly connected/adjacent nodes, S_{adj}, to initially ordered NFV nodes, shown in step 32, until all VNFs are

[3]To enable maximum bandwidth utilization and ensure that the disk space requirement of the VNF are satisfied.

successfully placed. For example, if $S_{adj} = 1$, the algorithm searches for NFV nodes directly connected to the initially selected NFV nodes, if no node is found, the value is We utilize the conditional statements in the algorithm to place the VNFs on the NFV nodes provided they satisfy their resource requirements and sufficient resources are available on the NFV nodes to host these VNFs.

Algorithm 1 VNF Migration algorithm

1: given: MEC network, represented as a graph of K NFV nodes
2: given: a set of VNFs $\mathbb{V} = \{v_1, v_2, \cdots, v_N\}$
3: given: CPU, RAM, BW, disk storage requirements of v_i (c_i, m_i, b_i, d_i)
4: given: max CPU, RAM, BW, disk storage capacities of NFV node (C, M_m, B_m, D_m)
5: define: load on s_j (L_i), load threshold of s_j (L_{th_j}), number of connected nodes (S_{adj}) to s_j
6: define: weight α in (0,1)
7: **procedure** VNF PLACEMENT
8: **while** $i \leq N$ **do**
9: **for** $n \leq S_{adj}$ **do**
10: **while** $j \leq K$ **do**
11: %calculate resource utilization
12: $U_{C_{ij}}, U_{M_{ij}}, U_{B_{ij}}, U_{D_{ij}}$
13: %calculate available resources
14: $C_{a_j} = C_{m_j} - U_{c_i}, M_{a_j} = M_{m_j} - U_{M_i}$
15: $B_{a_j} = B_{m_j} - U_{B_i}, D_{a_j} = D_{m_j} - U_{D_i}$
16: **if** $(U_{C_{ij}} \leq C_{a_j})$ & $(U_{M_{ij}} \leq M_{a_j})$
17: & $(U_{B_{ij}} \leq B_{a_j})$ & $(U_{D_{ij}} \leq D_{a_j})$ **then**
18: $L_j = \alpha_j U_{C_{ij}} + (1-\alpha_j) U_{M_{ij}} + U_{B_{ij}} + U_{D_{ij}}$
19: **if** $L_j \leq L_{th_j}$ **then**
20: assign v_i to s_j
21: $C_{m_j} = C_{a_j}$ & $M_{m_j} = M_{a_j}$,
22: $B_{m_j} = M_{a_j}$ & $D_{m_j} = D_{a_j}$
23: i = i+1, go to step 8
24: **else if** $L_j > L_{th_j}$ **then**
25: **if** α_i **then**
26: update α_i, go to step 10
27: **end if**
28: $j = j + 1$, go to step 9
29: **end if**
30: **else if** $(U_{C_{ij}} > C_{m_j})$ & $(U_{M_{ij}} > M_{m_j})$
31: & $(U_{B_{ij}} > B_{m_j})$ & $(U_{D_{ij}} > D_{m_j})$ **then**
32: $j = j + 1$, go to step 9
33: **end if**
34: **end while**
35: n = n+1
36: **end for**
37: i = i+1, go to step 8
38: **end while**
39: **end procedure**

IV. PERFORMANCE EVALUATION

We evaluate the performance of the proposed scheme, in one way, using simulations in terms of throughput, packet drop ratio for MNO, successful VNF placement ratio, load on NFV nodes, and revenue for operators. Also, an emulation tool has been used to evaluate the performance in terms of delay, throughput, and spectrum utilization.

A. SIMULATION ENVIRONMENT

The simulations are performed on a desktop computer with a 3.5 GHz quad-core computer with 16GB of RAM size. The simulations were performed using Pycharm 2022.3.2 IDE. The results are compared with those of the conventional scheme. In the conventional scheme, the MNOs operate on their individual licensed spectrum, and the MEC network is implemented based on the specification of ETSI [22], [23].

gNBs and MECs of three MNOs are deployed where the gNBs and MECs are assumed to be co–located. Each gNB has a coverage region of 200m. UEs are deployed randomly around each gNB, modeled as Poisson point processes. All MNOs share spectrum and MEC resources with each other. Also, UPF agents for MNOs are implemented as an application function for inter–operator communications. A set of services, implemented as VNFs, are offered to UEs. Each UE selects a service, i.e., a VNF, for a given time period measured in time slots (TS). UPF_G, of each MNO receives resource status updates including down-link throughput and channel state information, from other MNOs at specified intervals, at each TS. UPF_G estimates suitable gNB having sufficient resources to serve the UE. For this, if the average down-link throughput of the gNB and channel state values of available channels at a gNB, are above a threshold value, the gNB of that MNO is considered as candidate MNO. UPF_G sends suitable gNB information to the UE. Since we assume gNBs are co–located, if more than one gNB are selected, the UE estimates Reference Signal Received Power (RSRP), i.e, channel state information to the candidate gNBs, to select suitable gNB for sharing resources. {In the simulations, we model the channel between UEs and gNBs with Rayleigh distribution.

The algorithm works by acquiring channel state information for each UE to the gNB. This channel state information of UE has been utilized to select a gNB among the candidate gNBs list. Once a suitable gNB is selected, resources, i.e., spectrum and MEC resources, are shared by the concerned MNOs. The resource specifications of the considered VNFs are detailed in Table 2. We consider five different types of VNFs, i.e., authentication and file transfer protocol (FTP) [37], billing [38], firewall [39], and two transcoder type VNFs, i.e., OpenCV [40] and ffmpeg [41]. A mobile UE may receive service from any of these VNFs or a chain of these VNFs. For example, VNF1-VNF5 -VNF2, defines a video streaming service chain.

TABLE 2. Resource specifications for five different VNFs.

VNF name	VNF type	BW (Kbps)	DS (KB)	RAM (MB)	CPU (MHz)	Weight (α)
VNF1	auth/ftp	0.8K	20	16	1,15-50	[0.4-0.6]
VNF2	billing	0.8K	35	25	1,3500	[0.4-0.6]
VNF3	firewall	1K	200	250	1,3500	[0.4-0.6]
VNF4	OpenCV	3	175K	8192	1-4,3500	[0.6-0.8]
VNF5	ffmpeg	25K	175K	3860	1-4,3500	[0.6-0.8]

TABLE 3. Traffic profiles for different types of VNFs.

Parameter	Value
Traffic profile 1	
No. of channels for MNO 1 and 2	20,40,50
No. of UEs per MNO	10, 20, 30, 40, 50
VNF 1, 2, 3, 4, 5 durations	1, 1, 2, 3, 3 ms
VNF 1, 2, 3, 4, 5 channels	1, 1, 3, 5, 5
gNB buffer size	100 packets
Traffic profile 2	
No. of channels for MNO 1 and 2	20,40,50
No. of UEs per MNO	10, 20, 30, 40, 50
VNF 1, 2, 3, 4, 5 durations	1, 1, Poisson(λ=5), Pareto(β=1.4,ρ=1) , Pareto(β=1.4,ρ=1)ms
VNF 1, 2, 3, 4, 5 channels	1, 1, Poisson(λ=5,6,7,8), Pareto(β=1.4.1.3,1.2,1.1,ρ=1024), Pareto(β=1.4.1.3,1.2,1.1,ρ=1024)
gNB buffer size	100 packets

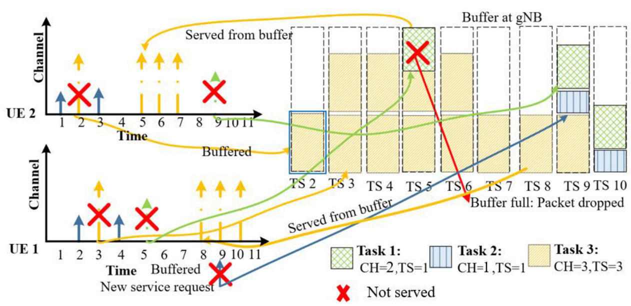

FIGURE 4. Example of traffic profiles for services (VNFs).

Two types of traffic profiles depending on the types of VNFs are considered. The parameter values considered for the two traffic profiles are represented in Table 3. For example, VNF types 1, 2, and 3, and VNFs 4 and 5 have different resources, i.e., channel and time slots, requirements. For example, in traffic profile 2, we consider, VNFs 1, 2, and 3 in Table 2 have Poisson arrival rates, and VNFs 4 and 5 have pareto type traffic arrivals [42]. Furthermore, it is assumed that each channel can serve only one packet and each time slot is 1ms. Each channel bandwidth is 1MHz and the channel is modeled using Rayleigh fading and log normal shadowing is considered.

An example of two types of traffic profiles is given in Fig. 4. Three different types of services have different resource requirements, indicated by Task 1, Task 2, and Task 3. When the resource requests received at the gNB are not greater than available resources, the resource request is served for the requested contiguous TS using the requested number

Timeslot	Action	Available Buffer: 7	Packet Status UE1	Packet Status UE2
1	UE2 served (CH=1, TS=1)	7		Served
2	UE1 served (CH=1, TS=1), UE2 request buffered (CH=3,TS=3)	4	Served	
3	UE 2 served (CH=1, TS=1), UE1 request buffered (CH=3,TS=3)	1		Served
4	UE1 served (CH=1, TS=1)	1		
5	UE2 request (CH=2,TS=1), UE2 request dropped, UE1 served from buffer	1	Served from buffer	Packet dropped buffer limit
6	No request, UE1 served from buffer	1	Served from buffer	
7	No request, UE1 served from buffer	1	Served from buffer	
8	No request, UE2 served from buffer	4		Served from buffer
9	UE1 request (CH=2,TS=1), UE1 request buffered, UE2 served from buffer	1		Served from buffer
10	UE2 served from buffer	4		buffer

FIGURE 5. gNB buffer status for the example in Fig. 4.

of channels; otherwise, it is buffered at the gNB queue. If a request is buffered and another request is received at that TS, the packets buffered earlier are served first and the new request is therefore buffered. Packets are dropped when the buffer at the gNB reaches its maximum limit. An explanation of the gNB buffer status under various traffic profiles is given in Fig. 5

The traffic profiles for VNF 4 and 5 are modeled as ON/OFF pareto distributions. During the ON–period,

$$P\{X < x\} = 1 - \left(\frac{\rho_p}{x}\right)^{\beta_p}, x > \rho_p, \tag{16}$$

where shape (β_p) = 1.05 and location (ρ_p) = 1024 bytes are parameters used to calculate the number of bytes of data generated during the ON–period. The size of each packet is set to 1024 bytes. Also,

$$P\{X < x\} = 1 - \left(\frac{\rho_t}{x}\right)^{\beta_t}, x > \rho_t, \tag{17}$$

where shape (β_t) = 1.4 and location (ρ_t) = 1 ms parameters are used to model the duration of OFF–period time slots. The parameters for pareto type traffic are selected based on traffic measurement and modeling in Fig. 5.

1) SIMULATION RESULTS

The proposed scheme has been evaluated in terms of average throughput under two different traffic profiles, average packet drop ratio for MNOs under varying simulation conditions, the successful VNF placements on NFV nodes, average load on NFV nodes on the MEC network, and the revenue opportunity for MNO under various network topologies.

The arrival rates of Poisson type traffic is increased for MNO A while the traffic arrival of MNO B is kept constant at λ=5. The corresponding throughput of MNOs with varying arrival rates is shown in Fig. 6. The number of channels and the number of UEs for both MNOs is kept same at 40 and 20, respectively. The proposed scheme shows higher throughput

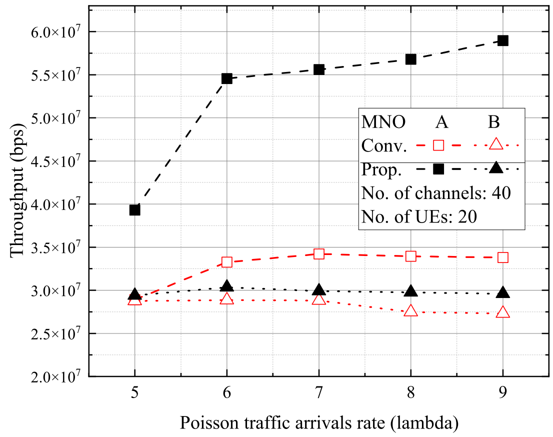

FIGURE 6. Throughput of MNO A and B with varying Poisson type traffic arrivals at MNO A and constant arrival rate at MNO B.

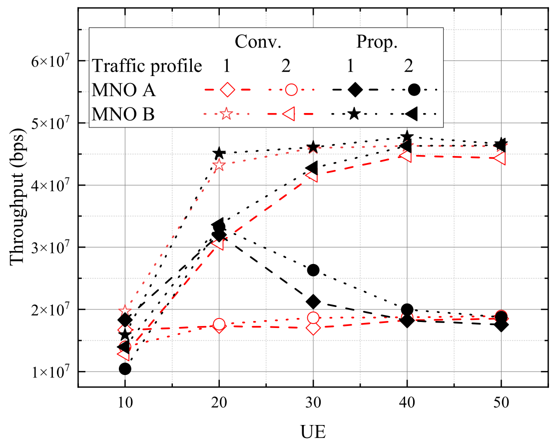

FIGURE 8. Average throughput of MNOs A and B. The number of channels for MNOs A and B are 20 and 40, respectively.

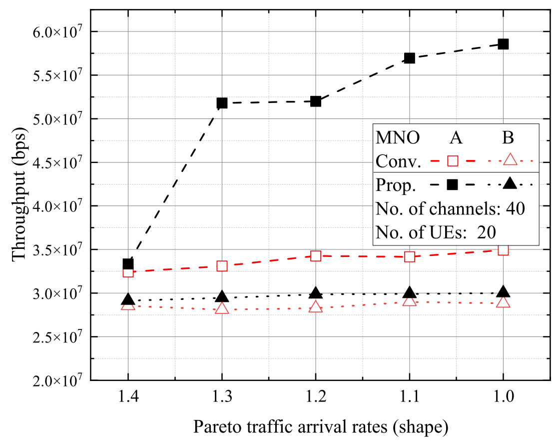

FIGURE 7. Throughput of MNO A and B with varying pareto type traffic arrivals at MNO A and constant arrival rate at MNO B.

compared to that of the conventional scheme for both MNOs. The throughput of MNO A for the proposed scheme, nearly increases linearly as it uses its own and other MNOs B resources. It becomes stable when the arrival rates are further increased at λ=7 because resources start to become scarce. In comparison, the throughput increases for MNO A for the conventional scheme but becomes stable at λ=6. This is because resources are not available to serve the users. Also, MNO B throughput nearly remains constant since its traffic arrival rate is constant.

The arrival rates of pareto type traffic vary for MNO A. The performance in terms of throughput is estimated for both MNOs in Fig. 7. The number of channels and the number of UEs for both MNOs is kept same at 40 and 20, respectively. The arrival rates for MNO B are kept constant at $\beta = 1.4$. The proposed scheme shows higher throughput compared to that of the conventional scheme for both MNOs. For the proposed scheme, the throughput for pareto type traffic does not increase linearly. It increases sharply and then becomes stable when arrival rate reaches $\beta = 1.1$. In comparison, the conventional scheme increases with increase in arrival rates up to $\beta = 1.2$. Since the MNO has A has limited resources, the throughput does not increase further. This is because, the number of packets queued in the buffer increase as traffic arrival rates increase. When the buffer reaches its limit, the upcoming packets are dropped.

The average throughput of MNO A and B are shown in Fig. 8. MNO A has lower number of available channels, therefore, it shares the spectrum resources with the MNO B and achieves higher throughput compared to that of the conventional scheme for both types of traffic profiles. MNO A throughput increases for UEs 20 and 30, and then becomes stable. This is because, initially, MNO A has available resources to share with MNO B, however, when its own requirement increases, it limits sharing resources with MNO A. Also, the throughput becomes stable when the number of UE goes to 30 since traffic intensity increases and packets are queued in the buffer. When the buffer becomes full, the packets are dropped. It is noted, for the proposed scheme, the throughput for MNO B is higher than conventional scheme, since it is sharing resources with MNO A. It is also observed that traffic profile 1 initially achieves higher throughput but as the number of UEs increases, the throughput for traffic profile 2 increases.

The packet drop ratio for MNOs with an increasing number of UEs is plotted in Fig. 9. The PDR for the conventional scheme is greater for both types of traffic profiles than that of the proposed spectrum sharing scheme. Also, the PDR for MNO A is greater since it does not have sufficient resources to serve its UEs when the number of UEs increases. Also, the PDR for traffic profile 1 is greater for the greater number of UEs, since more traffic is generated and thus leads to dropped packets as the traffic volume increase in the network. The traffic profile 2 OFF time, OFF TS, is modeled as pareto, therefore, the silent TS reduce the packet drop ratio especially when the number of UEs increase.

In addition, to evaluate the proposed VNF placement scheme,presented in Algorithm 1, we simulated it under two different topologies, as shown in Fig. 10. The topologies

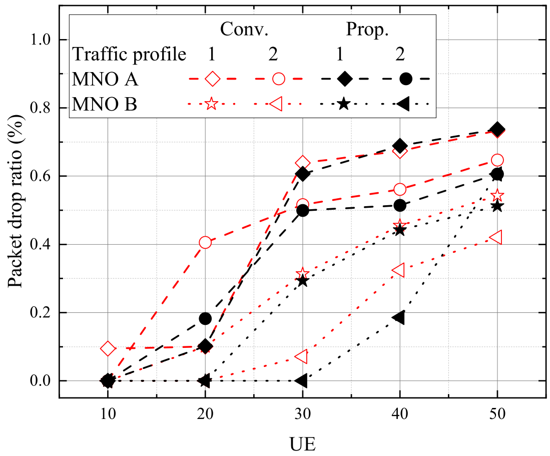

FIGURE 9. Average packet drop ratio of MNO A and MNO B. The number of channels for MNO A and B are 20 and 40, respectively.

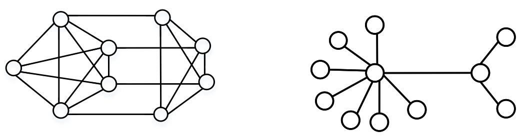

FIGURE 10. Networks topologies considered for MEC network.

TABLE 4. Average load on NFV nodes at the MEC network.

GridNet		Kreonet–s	
Prop.	Conv.	Prop.	Conv.
40.3082	48.3216	38.0764	52.2691

considered are extracted from Internet Topology Zoo [43]. The tests are repeated 1000 times in the simulation. The resource sharing requests are received from different candidate MNOs at the UPF_G.

The successful placements of these VNFs considering various loads on the NFV nodes, are shown in Fig. 11. It is observed that the number of placed VNFs increases with an increase in the load threshold values. The proposed scheme outperforms the conventional scheme because VNFs are placed on the servers considering their specific processing, memory, storage, and bandwidth requirements. All VNFs can be placed on the MEC nodes for the proposed scheme if the load threshold value is increased to 70%. In comparison, for the conventional scheme, the VNFs placement ratio is 20% smaller than the proposed scheme when the load threshold values are between 20% and 60%.

The average load on NFV nodes at the MEC network for different network topologies is shown in Table 4. The VNFs are placed on the NFV nodes considering the current load on the NFV nodes and the VNFs individual resource requirements, considering the specification detailed in Table 2. Consequently, the proposed scheme outperforms the conventional scheme and shows a smaller average load of 39% and 17% for the Kreonet–s and GridNet topology,

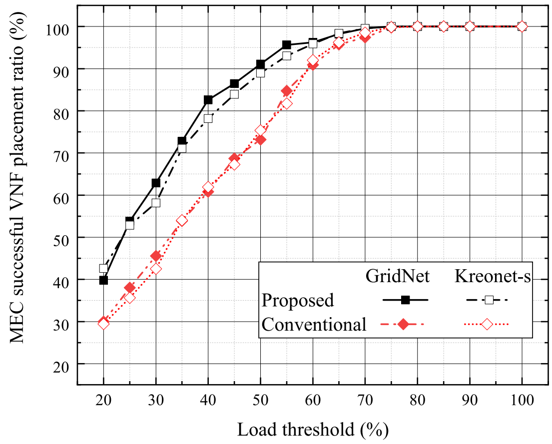

FIGURE 11. Number of successful VNFs placements on NFV nodes at MEC network.

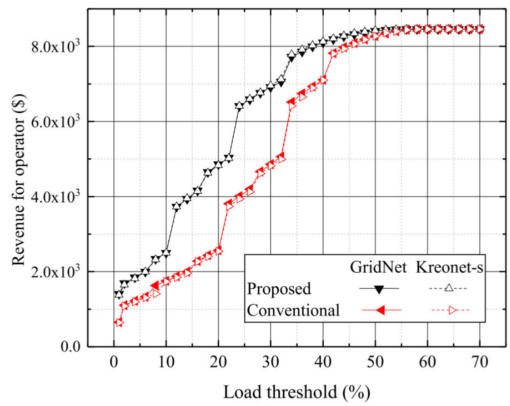

FIGURE 12. Revenue opportunity for MNO.

respectively. Furthermore, the proposed scheme maintains a nearly constant load on the NFV nodes, compared to that of the conventional scheme.

As shown in Fig. 12, the revenue for the operator for the proposed scheme is higher than the conventional scheme up to load threshold of 60%. The revenue is calculated based on pricing of each packet of VNF served by an MNO. The number of VNFs placements at the MEC are greater for the proposed scheme, therefore, more users receive their required services than the conventional scheme. This leads to greater revenue generation for the operator in the proposed scheme. At 60% load threshold, VNFs successful placement ratio becomes the same to that of the conventional scheme and generates similar revenues for both schemes.

B. EXPERIMENTAL ENVIRONMENT

We use the mininet emulation tool to implement a multi-operator cellular environment [44]. The experimental setup is shown in Fig. 13. The mininet topology is connected with multi RYU controllers setup as remote controllers, operating on the local computer. The other computer hosting the orchestrator for MNO B, is connected via LAN/internet. The

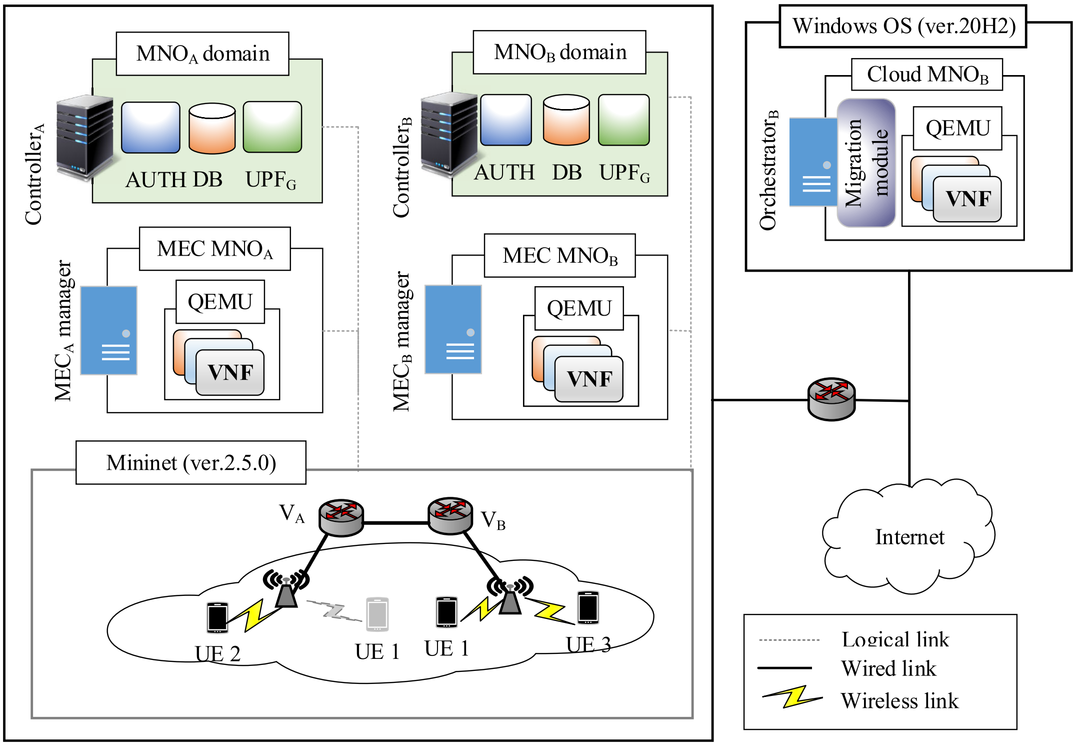

FIGURE 13. Emulation environment.

experiments were repeated 30 times. The domains for MNOs, consist of the SDN RYU controllers, and three modules. The authentication module (AUTH), a database module (DB), user plane function agent (UPF$_G$). A hashing table-based DB, implemented using a hashmap, contains connected UE's information such as UE IP address, connected access point (AP)'s service set identifier (SSID), MAC address of UEs, and UE's associated VNF list. The VNF list is determined by the service requested by the user. For example, VNF1-VNF3-VNF4-VNF2 could be a VNF list considering a transcoding type service offered to the user, following the VNFs presented in Table 2 of the manuscript. The AUTH module is responsible for authenticating a UE based on its MAC address, retrieved from the already stored information in the hashmap database. The UPF$_G$ is responsible for acquiring connected user information from the AP, and coordinating the migration of UE VNF information to other MNO. It also coordinates the migration of VNF from the cloud to the target MEC via python-based socket programming. Openflow and restful are used as the south-bound and north-bound application programming interfaces (APIs), respectively.

MECs of MNOs consist of a MEC manager, and QEMU virtualizer, for hosting the VNFs. These components are implemented on a desktop computer having a Ubuntu operating system (OS), version 18.04 LTS. The cloud network is implemented on a desktop computer having Windows 10 OS. It consists of the QEMU platform for hosting VNFs and an orchestrator to facilitate VNF migration. The two computers are connected using tunneling by defining the tap interface. This is achieved via defining a bridge adapter on computer hosting the orchestrator, therefore, the application programs communicate by obtaining a LAN address from the network, i.e., IP address from DHCP client. UE 1 is receiving service via VNF at MEC$_A$ and UE 2 creates the background traffic. All traffic is generated using the iPerf3 application using TCP transmissions [45]. TCP client is executing at UE 1 and receives traffic in the range of 5Mbps to 15Mpbs. UE 2 creates traffic in the range of 5Mbps to 25Mbps. The link capacity of BS$_A$ and BS$_B$ is 30Mbps. Also, the capacity of the link between switch V$_A$ and V$_B$ is 30Mbps. The proposed scheme is compared with the conventional scheme. In the conventional scheme the MNOs do not share resources. The conventional spectrum sharing scheme typically involves allocating specific frequency bands or channels to different users or services, such as mobile networks, categorized by exclusive spectrum usage, and dedicated licensed spectrum access shared among users.

1) EXPERIMENTAL RESULTS

The experimental setup was implemented to evaluate the performance of the proposed scheme, in terms of average delay and average throughput experienced by a UE, and the spectrum utilization of the MNO.

As shown in Fig. 14, up to 8s, UE 1 receives service from MNO A via AP. UE 2 dynamically generated large background traffic of 25Mbps at time 8s. In the interval from 9s to 14s, $Q \geq Q_{th}$, i.e., $\delta \geq \delta_{th}$. Since UE 1 is in the coverage region of new MNO, it connects to the AP of MNO$_B$. As the UE 1 connects to the AP, the migration function in UPF$_{G_B}$, is activated. The UE 1's associated VNF information is

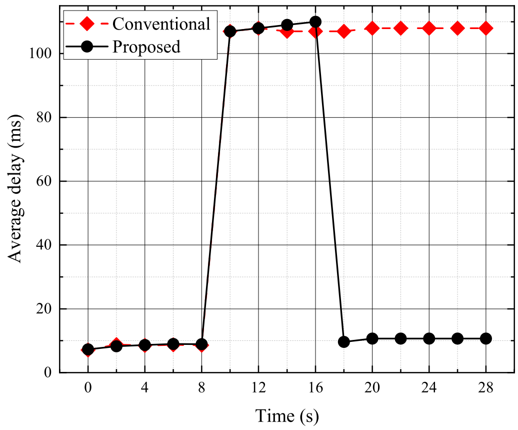

FIGURE 14. Average delay experienced by UE.

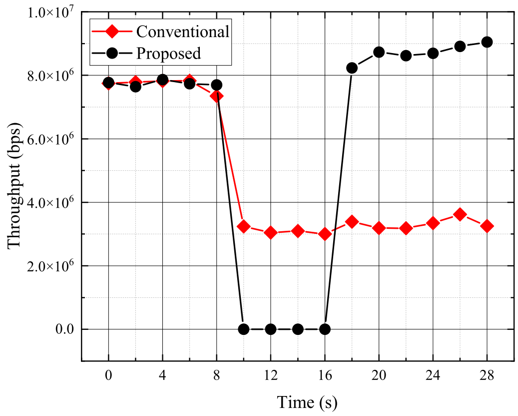

FIGURE 15. Average throughput experienced by UE.

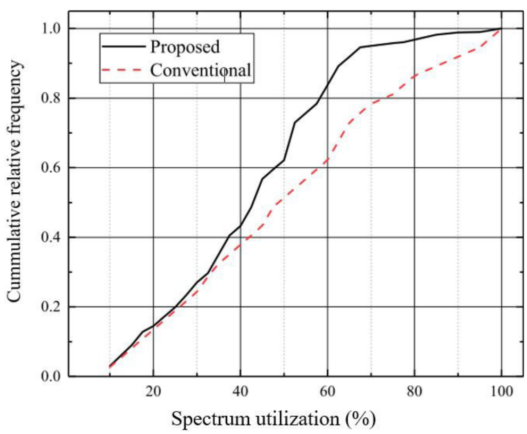

FIGURE 16. Cumulative relative frequency of spectral utilization (%) of MNO.

retrieved from UPF_{G_A} of MNO_A. The associated VNF is migrated from the cloud data network to the MEC_B during the interval 14s to 16s. New routing rules are created and UE 1 restores communication and the delay is reduced to 10ms approximately.

The average throughput for the UE is shown in Fig. 15. The UE 1 experiences a throughput of 8Mbps approximately, up to 8s. At this time, the background traffic increases up to 25Mbps, which results in low throughput. As explained earlier, the VNF is migrated, the controller at MNO_B creates new routing rules. Consequently, the throughput for the proposed scheme increases to 9Mbps. As a comparison, in the conventional scheme, the resources are not shared among MNOs, therefore, UE 1 experiences an average throughput of 3Mpbs.

The cumulative relative frequency of average spectrum utilization is shown in Fig. 16. We collect 30 samples of spectrum utilization to estimate the cumulative relative frequency. The proposed scheme has nearly the same performance in terms of spectrum utilization up to 40%, compared to that of the conventional scheme. In the proposed and conventional schemes, 97% and 85% of samples have spectrum utilization of less than 80%, respectively. Therefore, the proposed scheme has available spectrum resources more than the conventional one.

V. CONCLUSION

The complexity of the network situations, dynamicity of network environment, diverse services and user traffic demands make the conventional cellular technology unable to meet the requirements of eMBB, URLLC, and mMTC. In this paper we propose a multi-operator spectrum and MEC resource sharing scheme to overcome these limitations. Inter-operator communication was enabled via the newly introduced user plane function agent at the main cloud of the operator. This agent receives and manages resource sharing requests from other MNOs. A user receiving service using VNF at the edge network, may experience degraded performance due to lack of resources. This user can receive services from another MNO's MEC to maintain its QoS, within the coverage area under a shared resource environment scenario. In such a case, to offer service continuity, the associated VNF has to be migrated to the NFV node at the target MEC network. Following this, in our proposed scheme, firstly spectrum resource are shared with an operator with sufficient resources; secondly, the VNFs are migrated from the cloud data network and placed on the edge network considering the current load of the NFV nodes and individual resource requirements of VNFs. The proposed scheme has been evaluated using simulations and an emulation-based experimental setup. The results showed that the proposed scheme outperformed the conventional scheme in terms of network delay, network throughput, packet drop ratio, spectrum utilization, successful VNF placement ratio, load on edge nodes, and revenue for the operator.

CONFLICT OF INTEREST

There is no conflict of interest.

REFERENCES

[1] *Minimum Requirements Related To Technical Performance for IMT-2020 Radio Interface(s)*, document ITU-R M.2410-0, Int. Telecommun. Union, 2017. Accessed: Mar. 10, 2024. [Online]. Available: http://www.itu.int/publ/R-REP/en

[2] *Telecommunication Management; Network Sharing; Concepts and Requirements*, document 3GPP TS 32.130, Jun. 2016.

[3] M. Shirvanimoghaddam, M. Dohler, and S. J. Johnson, ''Massive non-orthogonal multiple access for cellular IoT: Potentials and limitations,'' *IEEE Commun. Mag.*, vol. 55, no. 9, pp. 55–61, Sep. 2017.

[4] H. Zhou, N. Cheng, Q. Yu, X. Sherman Shen, D. Shan, and F. Bai, ''Toward multi-radio vehicular data piping for dynamic DSRC/TVWS spectrum sharing,'' *IEEE J. Sel. Areas Commun.*, vol. 34, no. 10, pp. 2575–2588, Oct. 2016.

[5] P. Semasinghe, S. Maghsudi, and E. Hossain, ''Game theoretic mechanisms for resource management in massive wireless IoT systems,'' *IEEE Commun. Mag.*, vol. 55, no. 2, pp. 121–127, Feb. 2017.

[6] T. Taleb, K. Samdanis, B. Mada, H. Flinck, S. Dutta, and D. Sabella, ''On multi-access edge computing: A survey of the emerging 5G network edge cloud architecture and orchestration,'' *IEEE Commun. Surveys Tuts.*, vol. 19, no. 3, pp. 1657–1681, 3rd Quart., 2017.

[7] *Network Functions Virtualisation (NFV); Management and Orchestration*, Standard GS NFV-MAN 001, ETSI NFV, Dec. 2014.

[8] A. J. Gonzalez, G. Nencioni, A. Kamisinski, B. E. Helvik, and P. E. Heegaard, ''Dependability of the NFV orchestrator: State of the art and research challenges,'' *IEEE Commun. Surveys Tuts.*, vol. 20, no. 4, pp. 3307–3329, 4th Quart., 2018.

[9] Cisco. *Fog Computing, Ecosystem, Architecture and Applications*. Accessed: Jan. 4, 2024. [Online]. Available: http://www.cisco.com/web/about/ac50/ac207/crcnew/university/RFP/rfp13078.html

[10] F. Bonomi, R. Milito, J. Zhu, and S. Addepalli, ''Fog computing and its role in the Internet of Things,'' in *Proc. 1st Ed., MCC Workshop Mobile Cloud Comput.*, New York, NY, USA, Aug. 2012, pp. 13–16.

[11] A. De La Oliva, A. Banchs, I. Soto, T. Melia, and A. Vidal, ''An overview of IEEE 802.21: Media-independent handover services,'' *IEEE Wireless Commun.*, vol. 15, no. 4, pp. 96–103, Aug. 2008.

[12] M. Kassi and S. Hamouda, ''RAN virtualization: How hard is it to fully achieve?'' *IEEE Access*, vol. 12, pp. 38030–38047, 2024.

[13] L. Kundu, X. Lin, E. Agostini, V. Ditya, and T. Martin, ''Hardware acceleration for open radio access networks: A contemporary overview,'' *IEEE Commun. Mag.*, 2024.

[14] R. H. Tehrani, S. Vahid, D. Triantafyllopoulou, H. Lee, and K. Moessner, ''Licensed spectrum sharing schemes for mobile operators: A survey and outlook,'' *IEEE Commun. Surveys Tuts.*, vol. 18, no. 4, pp. 2591–2623, 4th Quart., 2016.

[15] T. Sanguanpuak, S. Guruacharya, N. Rajatheva, M. Bennis, D. Niyato, and M. Latva-Aho, ''Multi-operator spectrum sharing using matching game in small cells network,'' in *Proc. IEEE Int. Conf. Commun. (ICC)*, Kuala Lumpur, Malaysia, May 2016, pp. 1–6.

[16] B. Singh, K. Koufos, O. Tirkkonen, and R. Berry, ''Co-primary inter-operator spectrum sharing over a limited spectrum pool using repeated games,'' in *Proc. IEEE Int. Conf. Commun. (ICC)*, Jun. 2015, pp. 1494–1499.

[17] S. K. Joshi, K. B. S. Manosha, M. Codreanu, and M. Latva-Aho, ''Dynamic inter-operator spectrum sharing via Lyapunov optimization,'' *IEEE Trans. Wireless Commun.*, vol. 16, no. 10, pp. 6365–6381, Oct. 2017.

[18] P. Luoto, M. Bennis, P. Pirinen, S. Samarakoon, and M. Latva-Aho, ''Enhanced co-primary spectrum sharing method for multi-operator networks,'' *IEEE Trans. Mobile Comput.*, vol. 16, no. 12, pp. 3347–3360, Dec. 2017.

[19] C. Liang and F. R. Yu, ''Wireless network virtualization: A survey, some research issues and challenges,'' *IEEE Commun. Surveys Tuts.*, vol. 17, no. 1, pp. 358–380, 1st Quart., 2015.

[20] M. Silva, J. Santos, and M. Curado, ''The path towards virtualized wireless communications: A survey and research challenges,'' *J. Netw. Syst. Manage.*, vol. 32, no. 1, p. 12, Jan. 2024.

[21] X. Costa-Perez, J. Swetina, T. Guo, R. Mahindra, and S. Rangarajan, ''Radio access network virtualization for future mobile carrier networks,'' *IEEE Commun. Mag.*, vol. 51, no. 7, pp. 27–35, Jul. 2013.

[22] *Multi-Access Edge Computing (MEC); Technical Requirements*, Standard ETSI GS MEC 002 V2.1.1, Oct. 2018.

[23] *Mobile Edge Computing (MEC). In Framework and Reference Architecture*, Standard ETSI GS MEC 003 V1.1.1, ETSI, Valbonne, France, Mar. 2016.

[24] Y. C. Hu, M. Patel, D. Sabella,N. Sprecher, and V. Young, ''Mobile edge computing: A key technology towards 5G,'' ETSI, Valbonne, France, White Paper 11, 2015.

[25] M. Bennis, M. Debbah, and H. V. Poor, ''Ultrareliable and low-latency wireless communication: Tail, risk, and scale,'' *Proc. IEEE*, vol. 106, no. 10, pp. 1834–1853, Oct. 2018.

[26] P. Porambage, J. Okwuibe, M. Liyanage, M. Ylianttila, and T. Taleb, ''Survey on multi-access edge computing for Internet of Things realization,'' *IEEE Commun. Surveys Tuts.*, vol. 20, no. 4, pp. 2961–2991, 4th Quart., 2018.

[27] P. Mach and Z. Becvar, ''Mobile edge computing: A survey on architecture and computation offloading,'' *IEEE Commun. Surveys Tuts.*, vol. 19, no. 3, pp. 1628–1656, 3rd Quart., 2017.

[28] A. C. Baktir, A. Ozgovde, and C. Ersoy, ''How can edge computing benefit from software-defined networking: A survey, use cases, and future directions,'' *IEEE Commun. Surveys Tuts.*, vol. 19, no. 4, pp. 2359–2391, 4th Quart., 2017.

[29] I. Afolabi, T. Taleb, K. Samdanis, A. Ksentini, and H. Flinck, ''Network slicing and softwarization: A survey on principles, enabling technologies, and solutions,'' *IEEE Commun. Surveys Tuts.*, vol. 20, no. 3, pp. 2429–2453, 3rd Quart., 2018.

[30] *Network Functions Virtualisation (NFV)—Virtual Network Functions Architecture*, ETSI, ISG, Sophia Antipolis, France, 2013.

[31] E. Haleplidis, J. H. Salim, S. Denazis, and O. Koufopavlou, ''Towards a network abstraction model for SDN,'' *J. Netw. Syst. Manage.*, vol. 23, no. 2, pp. 309–327, Apr. 2015.

[32] *Technical Specification Group Services and System Aspects; System Architecture for the 5G System; Stage 2, Release 15*, document 3GPP TS 23.501, Version 15.0.0, 3rd Generation Partnership Project, Dec. 2017. [Online]. Available: http:/www.3gpp.org/ftp/Specs/archive/23_series/23.501/23501-f00.zip

[33] *Viava Observer (v18) and GigaStor (Gen4)*. Accessed: Jan. 20, 2024. [Online]. Available: https://www.viavisolutions.com/en-us

[34] Microsoft Azure. *Content Delivery Network Pricing*. Accessed: Dec. 16, 2023. [Online]. Available: https://azure.microsoft.com/en-us/pricing/details/cdn/

[35] Y. Yamato, ''Server selection, configuration and reconfiguration technology for IaaS cloud with multiple server types,'' *J. Netw. Syst. Manage.*, vol. 26, no. 2, pp. 339–360, Apr. 2018.

[36] W. Attaoui, E. Sabir, H. Elbiaze, and M. Guizani, ''VNF and CNF placement in 5G: Recent advances and future trends,'' *IEEE Trans. Netw. Service Manage.*, vol. 20, no. 4, pp. 4698–4732, Dec. 2023.

[37] *TinyCore/Linux*. Accessed: Jan. 16, 2024. [Online]. Available: http://www.tinycorelinux.com/

[38] *GNU/Linux*. Accessed: Jan. 16, 2024. [Online]. Available: http://www.slitaz.org/

[39] *OpenWRT*. Accessed: Jan. 16, 2024. [Online]. Available: https://openwrt.org/

[40] A. Kaehler and G. Bradski, *Learning OpenCV 3: Computer Vision in C++ With the OpenCV Library*. Sebastopol, CA, USA: O'Reilly Media, 2016.

[41] F. Bellard. *FFMPEG*. Accessed: Jan. 16, 2022. [Online]. Available: https://www.ffmpeg.org/

[42] W. E. Leland, W. Willinger, M. S. Taqqu, and D. V. Wilson, ''On the self-similar nature of Ethernet traffic,'' *ACM SIGCOMM Comput. Commun. Rev.*, vol. 25, no. 1, pp. 202–213, Jan. 1995.

[43] The University of Adelaide, Adelaide, SA, Australia. *The Internet Topology Zoo*. Accessed: Jan. 15, 2024. [Online]. Available: http://www.topology-zoo.org

[44] *Open Networking Foundation (ONF)*. Accessed: Jan. 16, 2024. [Online]. Available: https://www.opennetworking.org/

[45] M. Mortimer et al., ''French iPerf forum, iPerf3 documentation, release 0.1.10,'' Tech. Rep., 2018.

TAHIRA MAHBOOB (Member, IEEE) received the B.S. degree in computer science and engineering and the M.S. degree in computer engineering from the University of Engineering and Technology, Pakistan, in 2007 and 2012, respectively, and the Ph.D. degree in computer engineering from Sungkyunkwan University, Republic of Korea, in 2022. She is currently an Assistant Professor with the Department of Computer and Software Engineering, Information Technology University of the Punjab, Pakistan. She was a Postdoctoral Fellow with Kyung Hee University, Republic of Korea. From 2010 to 2018, she was a Faculty Member of Fatima Jinnah Women University, Pakistan. Her research interests include software-defined networking (SDN), network function virtualization (NFV), 5G and beyond communication networks, deep learning, and AI-enabled communication networks.

SYED TARIQ SHAH received the master's and Ph.D. degrees from the Department of Electrical and Electronic Engineering, Sungkyunkwan University, Republic of Korea, in 2015 and 2018, respectively. He is currently a Distinguished Academic and Researcher in the field of electrical and electronic engineering. Following the Ph.D. degree, he contributed significantly to the field as a Postdoctoral Fellow with the University of Glasgow, U.K., and took on the role of an Associate Professor with the Department of Electrical Engineering, BUITEMS, Pakistan. Currently, he holds the position of a Lecturer with the School of Computer Science and Electronic Engineering (CSEE), University of Essex, where he continues to advance research areas including 5G and beyond networks, open RAN, AI-enabled communication networks, RF energy harvesting, and intelligent reflective surfaces. An active member of the academic community, he serves as an Editor for the *Electronics* journal and is a respected reviewer for several IEEE TRANSACTIONS, letters, and magazines, contributing his expertise to shape the future of telecommunications and electronic engineering.

MINSEOK CHOI (Member, IEEE) received the B.S., M.S., and Ph.D. degrees from the School of Electrical Engineering, Korea Advanced Institute of Science and Technology (KAIST), Daejeon, South Korea, in 2011, 2013, and 2018, respectively. He has been with Kyung Hee University, Yongin, South Korea, since 2022. He is currently an Assistant Professor. He was a Visiting Postdoctoral Researcher in electrical and computer engineering with the University of Southern California (USC), Los Angeles, CA, USA, and a Research Professor in electrical engineering with Korea University, Seoul, South Korea. He was an Assistant Professor with Jeju National University, Jeju, South Korea, from 2020 to 2022. His research interests include federated learning, wireless caching networks, and AI-based network optimization. He was a recipient of IEEE ComSoc MMTC Best Journal Paper Award, in 2021.

SANG-HYO KIM (Member, IEEE) received the B.Sc., M.Sc., and Ph.D. degrees in electrical engineering from Seoul National University, Seoul, South Korea, in 1998, 2000, and 2004, respectively. From 2004 to 2006, he was a Senior Engineer with Samsung Electronics. He was with the University of Southern California, Los Angeles, CA, USA, as a Visiting Scholar, from 2006 to 2007. In 2007, he joined the College of Information and Communication Engineering, Sungkyunkwan University, Suwon-si, South Korea, where he is currently a Professor. In 2015, he had a one-year visit to the University of California at San Diego, San Diego, CA, USA, as a Visiting Scholar. His research interests include coding theory, wireless communications, and deep-learning-based communication systems. He has served as an Editor for *Transactions on Emerging Telecommunications Technologies* and *Journal of Communications and Networks*, in 2013.

MIN YOUNG CHUNG (Member, IEEE) received the B.S., M.S., and Ph.D. degrees in electrical engineering from Korea Advanced Institute of Science and Technology, Daejeon, South Korea, in 1990, 1993, and 1999, respectively. From January 1999 to February 2002, he was a Senior Member of Technical Staff with the Electronics and Telecommunications Research Institute, where he was engaged in research on the development of multiprotocol label switching systems. In March 2002, he joined as a Faculty Member of Sungkyunkwan University, Suwon-si, South Korea, where he is currently a Professor with the Department of Electrical and Computer Engineering. His research interests include D2D communications, software-defined networking (SDN), 5G wireless communication networks, and wireless energy harvesting. He worked as an Editor on the *Journal of Communications and Networks*, from January 2005 to February 2011; and is a member of IEICE, KICS, KIPS, and KISS.